On the Preferred Orientation and Microstructural Manipulation of Molecular Sieve Films Prepared by Secondary Growth

Anastasios Gouzinis and Michael Tsapatsis*

Department of Chemical Engineering, Goessmann Laboratory, University of Massachusetts Amherst, Amherst, Massachusetts 01003

Received April 2, 1998. Revised Manuscript Received June 2, 1998

MFI-supported films were prepared using secondary growth of precursor layers. The precursor layers were prepared free of additives and no calcination step was used before secondary growth. Combined microstructural control over film thickness, orientation, continuity, and surface roughness was achieved. Hydrothermal conditions were identified, such as film growth proceeds predominantly by direct growth of the particles of the precursor layer. The prepared polycrystalline films have a columnar microstructure. The out-of-plane grain orientation can be manipulated by secondary growth conditions, and is such that the *c*-axes of the grains range from perpendicular to the substrate to an angle of ∼34° from the direction normal to the substrate, whereas the in-plane grain orientation is random. Initial film growth rates were sustained at a constant value for extended periods of time with an activation energy of 70 kJ/mol. The degree of out-of-plane orientation increases with film thickness up to a point where changes in concentrations in the secondary growth solution lead to surface roughening and change in the preferred growth direction. Sustained growth preserving film orientation and columnar microstructure is achieved during repeated secondary growth, allowing for control of the film thickness without compromising the deposit orientation and surface smoothness. As a result of their microstructure exhibiting well-intergrown columnar texture with small surface roughness, oriented films with thickness well exceeding the wavelength of visible light are optically transparent.

1. Introduction

Zeolite films have attracted considerable interest due to their potential use in several applications, including selective membranes, electrodes, sensors, and optoelectronic devices.[1−9] For applications such as selective membranes, which need to utilize the molecular sieving properties of these materials, the ideal configuration would be a thin, appropriately oriented zeolite layer without interzeolitic porosity.

Zeolite membrane preparation has been reported for several different types of zeolites using, mainly, in situ techniques.[10−19] Preferentially oriented molecular sieve membranes have been reported recently.[20,21]

The issue of microstructural evolution during oriented film formation is addressed only in a limited number of reports. Jansen and Rosmalen[22] reported preparation conditions that can lead to oriented and intergrown MFI layers, supported on silicon wafers. Altering the synthesis conditions, Jansen et al.[23] were able to obtain similar films without interzeolitic porosity visible by scanning electron microscopy (SEM). Koegler et al.[24] further investigated this preparation technique and proposed a growth mechanism for this type of synthesis. According to this mechanism, a thin gel layer is formed

* Corresponding author. E-mail: tsapatsi@ecs.umass.edu.

(1) Yan, Y.; Bein, T. *J. Am. Chem. Soc.* **1995**, *117*, 9990.
(2) Yan, Y.; Bein, T. *J. Phys. Chem.* 1992, *96*, 9387.
(3) Yan, Y.; Bein, T. *Chem. Mater.* 1992, *4*, 975.
(4) Bein, T.; Brown, K. *J. Am. Chem. Soc.* **1989**, *111*, 7641.
(5) Caro, J.; Finger, G.; Kornatowski, J.; Mendau, J. R.; Werner, L.; Zibrowius, B. *Adv. Mater.* **1992**, *4*, 273.
(6) Ozin, G. A.; Kuperman, A.; Stein, A. *Angew. Chem., Int. Ed. Engl.* **1989**, *28*, 359.
(7) Stein, A. M.Sc. Thesis, University of Toronto, 1988.
(8) Frei, H.; Blatter, F.; Sun, H. *Chemtech* **1996**, 24.
(9) Laine, P.; Seifert, R.; Giovanoli, R.; Calzaferri, G. *New J. Chem.* **1997**, *21*, 453.
(10) Anderson, M. W.; Pachis, S. K.; Shi, J.; Carr, S. W. *J. Mater. Chem.* **1992**, *2*, 255.
(11) Sano, T.; Mizukami, F.; Takaya, H.; Mouri, T.; Watanabe, M. *Bull. Chem. Soc. Jpn.* **1992**, *65*, 146.
(12) Tsikoyiannis, J. G.; Haag, W. O. *Zeolites* **1992**, *12*, 126.
(13) Geus, E. R.; Bekkum, H.; Bakker, W. J. W.; Moulijn, J. A. *Microporous Mater.* **1993**, *1*, 131.
(14) Noble, R. D.; Falconer, J. L. *Catal. Today* **1995**, *25*, 209.
(15) Vroon, Z. A. E. P.; Keizer, K.; Gilde, M. J.; Verweij, H.; Burggraaf, A. J. *J. Membr. Sci.* **1996**, *113*, 293.
(16) Yan, Y.; Tsapatsis, M.; Gavalas, G. R.; Davis, M. E. *J. Chem. Commun.* **1995**, 227.
(17) Kapteijn, F.; Bakker, W. J. W.; Zheng, G.; Poppe, J.; Moulijn, J. A. *Chem. Eng. J.* **1995**, *57*, 145.
(18) Bakker, W. J. W.; Kapteijn, F. P. J.; Moulijn, J. A. *J. Membr. Sci.* **1996**, *117*, 57.
(19) Kusakabe, K.; Kuroda, T.; Murata, A.; Morooka, S. *Ind. Eng. Chem. Res.* **1997**, *36*, 649.
(20) Lovallo, M. C.; Tsapatsis, M. *AIChE J.* **1996**, *42*, 3020.
(21) Lovallo, M. C.; Gouzinis, A.; Tsapatsis, M. *AIChE*. In press.
(22) Jansen, J. C.; Rosmalen, G. M. *J. Cryst. Growth* **1993**, *128*, 1150.
(23) Jansen, J. C.; Kashchiev, D.; Erdem-Senatalar, A. In *Advanced Zeolite Science and Applications*; Jansen, J. C., Stocker, M., Karge, H. G., Weitkamp, J., Eds.; Elsevier Science: Amsterdam, 1994; pp 215−250.
(24) Koegler, J. H.; Bekkum, H.; Jansen, J. C. *Zeolites* **1997**, *19*, 262.

S0897-4756(98)00240-3 CCC: $15.00
Published on Web 08/13/1998

on the substrate (silicon wafers) and nucleation occurs at the gel/solution interface. Crystal growth proceeds into the gel phase until the crystals bond with the support and finally align with their (010) faces parallel to the substrate.

The gel formation was also observed by Kiyozumi et al.[25] during the formation of MFI noncomposite films on mercury surfaces. The film side that was in contact with the mercury had crystal orientation with the (0*k*0) and/or (*h*00) crystal planes parallel to the film surface, according to the X-ray diffraction (XRD) patterns. On the other hand, the solution side of the films had random orientation. The SEM images show that the films are formed with crystals that are well intergrown, and the final films appear transparent under optical observation. These properties are attributed to the use of the nonsolid support. It is suggested by the authors that mercury fluctuation generates a capillary wave that contributes to a moderate shaking of the crystals, providing an additional driving force for intergrowth. As a result, uniform and smooth films were obtained.

Tsapatsis and co-workers[26] proposed the secondary growth technique for the preparation of molecular sieve films. The processing scheme consists of using a colloidal zeolite suspension to form a precursor layer on a substrate. This step is followed by the secondary growth step, which involves crystal growth of the precursor layer particles to eliminate intercrystalline porosity.[20,21,26−31] Using the secondary growth technique for the preparation of MFI films, it was demonstrated that the prepared films exhibit orientation such that the crystals were preferentially oriented with their *c*-axis nearly perpendicular to the substrate.[20,21,31]

Secondary growth of seed layers was also employed by Valtchev et al.,[32] Mintova et al.,[33] and Hedlund et al.[34] for the preparation of ultrathin silicalite films on nonporous substrates. The substrate is modified to facilitate adsorption of a monolayer of small zeolite seed crystals, whereafter seeded growth leads to an intergrown film. Hedlund et al.[34] stated that depending on the size of the seed crystals, the final film thickness might vary from 110 to 720 nm. However, no preferential orientation was demonstrated for MFI films in these reports.

In another report, Mintova et al.[35] used the seed layer technique to further investigate the formation of intergrown MFI films on modified gold surfaces. Based on XRD, a preferential orientation of the crystals in the precursor layer is claimed, with the (0*1*0) faces parallel to the surface. However, as the films grow thicker, during secondary growth, almost all reflections of the MFI structure are present in the X-ray pattern, indicating nearly random orientation.

In the work just described, binders or additives were used for the preparation of the precursor layer[20,21] along with modification of the substrate by organic or inorganic coatings[32−35] to ensure high coverage and attachment of the zeolite seed nanoparticles on the substrate. Furthermore, before secondary growth, calcination of the precursor layer was applied to enhance adhesion of particles to the substrate.

In what follows, it is demonstrated that the use of elevated temperatures and/or additives is not necessary for the preparation of the precursor layer. In section 3.1 it is shown that by secondary growth at 175 °C a *c*-axis out-of-plane preferential orientation is achieved and that the degree of out-of-plane orientation increases with film thickness. In section 3.2 it is demonstrated that the out-of-plane orientation can be manipulated by varying the temperature of secondary growth. A speculation for the reason leading to different orientation is also presented in this section. In section 3.3 it is established that renewal of reactants during secondary growth can lead to sustained film growth, preserving and enhancing the preferred orientation. Finally, in section 3.4, the preparation of transparent and oriented MFI films is reported. The transparency is attributed to the grain structure and small surface roughness of thick films prepared by sustained growth.

2. Experimental Section

2.1. Preparation. A colloidal silicalite suspension with discrete particles (∼100 nm), concentration of 15 g/L, and pH ∼ 8 was prepared as previously reported,[20] but excluding the use of the alumina binder. The suspension was used for coating nonporous substrates (glass slides) with a precursor layer. The substrates were left to dry in air at room temperature overnight and further dried for 2 h at 50 °C. Then they were placed vertically in Teflon-lined reaction vessels. Subsequently, they were treated hydrothermally (*secondary growth*) at 175 and 140 °C using a solution with a composition of $40SiO_2$:9TPAOH:$9500H_2O$:160EtOH to obtain MFI films.

2.2. Characterization. X-ray diffraction was used to characterize the orientation of the obtained films. The XRD patterns were collected on a Phillips X'Pert system using Cu Kα radiation. X-ray powder diffraction was performed in a $\theta/2\theta$ geometry. For this type of analysis, crystal planes that are parallel to the substrate are detected and, for relatively thick films, this is the technique of choice for preliminary analysis of preferred orientation. X-ray thin film analysis was also used with the angle of incidence set to 1° for characterization of the precursor layers and films at the early stages of secondary growth. The XRD pole figure was used to quantify the degree of the orientation achieved. For these measurements, the 2θ positions of the desired reflections were identified from the powder XRD pattern. The incidence and exit angle were fixed at this position and the sample was rotated 360° (φ) for each tilt angle (ψ).

Scanning electron microscopy (SEM) was performed on a JEOL 100CX microscope operating in SEM mode at 20 kV.

(25) Kiyozumi, Y.; Mizukami, F.; Maeda, K.; Kodzasa, T.; Toba, M.; Niwa, S. *Stud. Surf. Sci. Catal.* **1997**, *105*, 2225.
(26) Tsapatsis, M.; Okubo, T.; Lovallo, M.; Davis, M. E., In *Advances in Porous Materials*; Komarneni, S., Smith, D. M., Beck, J. S., Eds.; Materials Research Society: Pittsburgh, 1995; Vol. 371; p 21.
(27) Lovallo, M. C.; Tsapatsis, M.; Okubo, T. *Chem. Mater.* **1996**, *8*, 1579.
(28) Tsapatsis, M.; Lovallo, M. C.; Okubo, T.; Davis, M. E.; Sadakata, M. *Chem. Mater.* **1995**, *7*, 1734.
(29) Lovallo, M. C.; Boudreau, L. C.; Tsapatsis, M., In *Microporous and Macroporous Materials*; Beck, J. S., Iton, L. E., Corbin, L. E., Lobo, R. F., Davis, M. E., Zones, S. I., Suib, S. L., Eds.; Materials Research Society: Pittsburgh, 1996; pp 225−236.
(30) Boudreau, L. C.; Tsapatsis, M. *Chem. Mater.* **1997**, *9*, 1705.
(31) Lovallo, M. C.; Tsapatsis, M. In *Advanced Catalytic Materials III*; Lednor, P., Ledoux, M., Nagaki, D., Thompson, L., Eds.; Materials Research Society: Pittsburgh, PA, in press.
(32) Valtchev, V.; Schoeman, B. J.; Hedlund, J.; Mintova, S.; Sterte, J. *Zeolites* **1996**, *17*, 408.
(33) Mintova, S.; Hedlund, J.; Schoeman, B.; Valtchev, V.; Sterte, J. *Chem. Commun.* **1997**, 15.
(34) Hedlund, J.; Schoeman, B. J.; Sterte, J. *Stud. Surf. Sci. Catal.* **1997**, *105*, 2203.
(35) Mintova, S.; Valtchev, V.; Engstrom, V.; Schoeman, B. J.; Sterte, J. *Microporous Mater.* **1997**, *11*, 149.

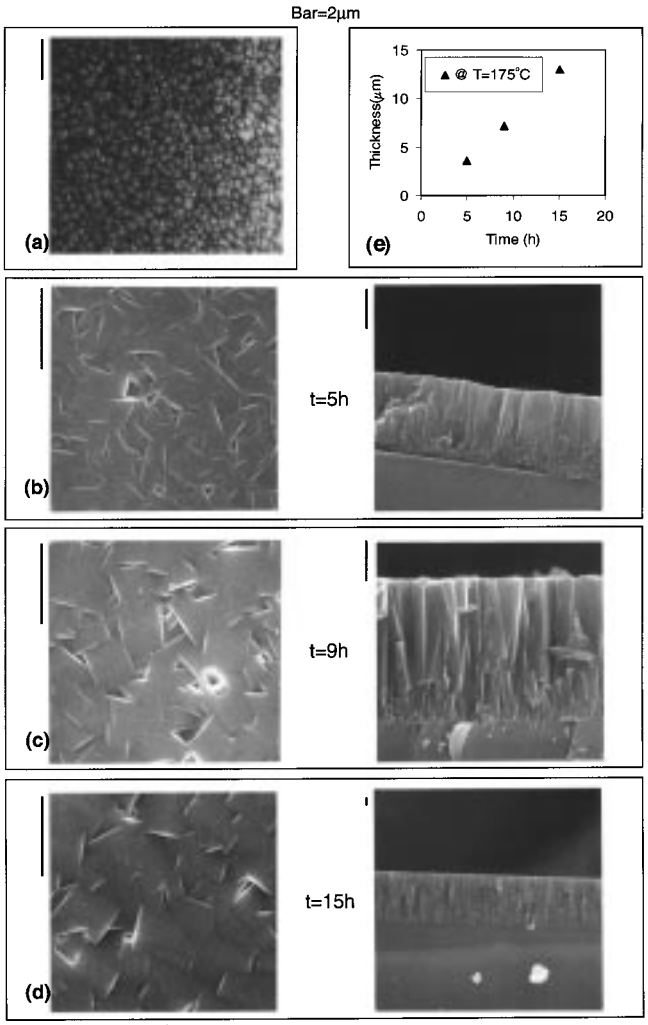

Figure 1. SEM micrographs of (a) the precursor layer and after secondary growth at 175 °C for (b) 5 h, (c) 9 h, and (d) 15 h; (e) film thickness versus secondary growth time.

The samples were mounted on the specimen holder with conductive carbon tape and sputtered with a gold coating.

3. Results and Discussion

3.1. Microstructural Evolution for Secondary Growth at 175 °C. The film microstructure evolution during secondary growth was followed by SEM and XRD. Figures 1b−d show SEM top views and corresponding cross sections for films prepared by secondary growth at 175 °C. Film thickness evolution is followed from 0 to 15 h (Figure 1e). Figure 2 shows the corresponding $\theta/2\theta$ diffractograms for up to 15 h of secondary growth, and Figure 3 shows X-ray pole figures for films obtained after 5 and 15 h of secondary growth.

Before the secondary growth step, the precursor layer is comprised of nearly a monolayer of silicalite nanocrystals. The interpenetrant twin nanoparticles exhibit equiaxed morphology, shown in the SEM top view of Figure 1a. Their nearly spherical shape results in a random orientation of the precursor particles. The thin film XRD pattern shown in Figure 2a indicates the absence of preferential orientation in the precursor layer.

Despite the random orientation of the precursor layer, a preferentially oriented film is obtained upon secondary growth. Deviations from random orientation are already apparent after 5 h of secondary growth at 175 °C (Figure 2b) and are strongly manifested after 9 and 15 h (Figures 2c and d, respectively). Some of the reflections that are clearly resolved in the precursor layer pattern (Figure 2a) decrease in intensity, but after 5 h of secondary growth (Figure 2b), the reflections corresponding to the (*h*0*l*) or (0*hl*) crystal planes dominate the pattern. In addition, the intensity of the (002) reflection increases. This reflection is weak for the precursor layer, but after 15 h of secondary growth (Figure 2d) has the highest relative intensity. These results show a preferred orientation where a large fraction of the crystals have their *c*-axis perpendicular to the substrate, whereas the rest are slightly tilted around the direction normal to the substrate. The deviations from random orientation, as revealed from XRD, coincide with the appearance and pronounced development of columnar texture shown in the SEM cross sections of Figure 1 (Figures 1b to 1d). It can be concluded that the long axis of the columnar grains of the polycrystalline MFI films prepared by secondary growth at 175 °C is their *c*-axis.

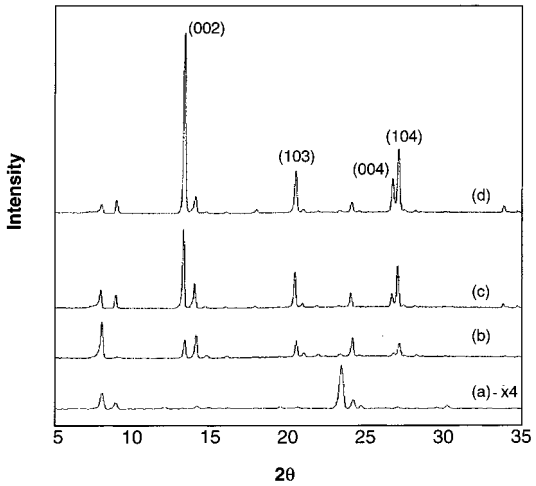

Figure 2. Thin film XRD pattern of the (a) precursor layer, and XRD patterns after secondary growth at 175 °C for (b) 5 h, (c) 9 h, and (d) 15 h.

Additional X-ray pole figure analysis was performed for the films obtained after 5 and 15 h of secondary growth at 175 °C. The analysis was carried out for the (002) and (101) or (011) reflections. Spinning the sample from 0 to 360° did not affect the diffracted intensity. This result can be seen in Figure 3a, where a quadrant of the (101) pole figure is presented for the film obtained after 15 h of secondary growth. This result was also observed in a previous report[31] and indicates a random rotation of the crystals around the axis normal to the substrate (i.e., random in-plane orientation). For this reason, the pole figure line plots presented in Figure 3b are sufficient to describe the orientational order of the films. As can be seen from this figure, the intensity of the (002) line plot has a maximum at 0° tilt angle for both samples, as was expected because for crystals that are *c*-oriented, the (00*l*) planes are parallel to the substrate surface. For the film obtained after 15 h of secondary the intensity maximum at 0° is sharper compared with the one obtained after 5 h. Furthermore, the intensity drops

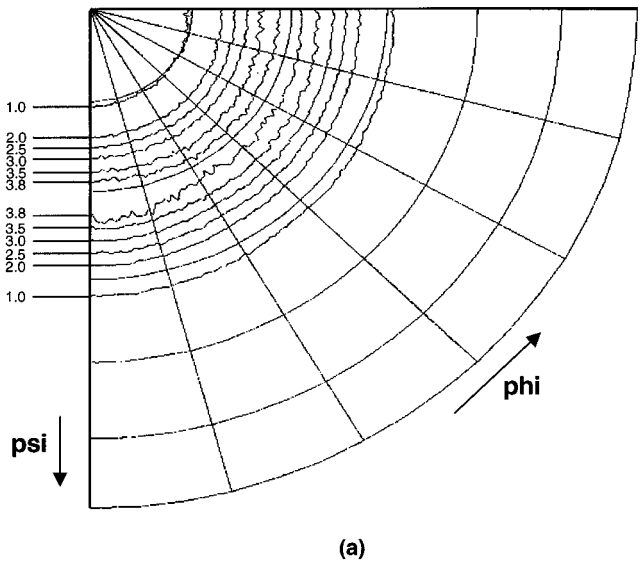

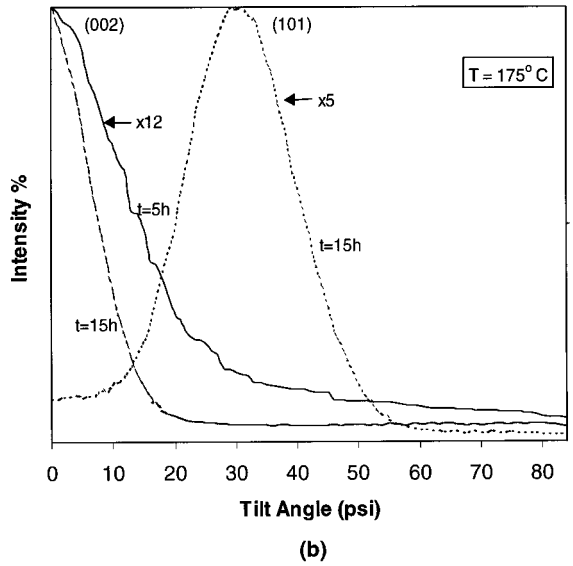

Figure 3. (a) Quadrant of the (101) pole figure for the film obtained after secondary growth at 175 °C for 15 h. (b) Pole figure line plots of films obtained after secondary growth at 175 °C for 5 and 15 h.

essentially to zero at high tilt angles. The (101) line plot from the film obtained after 15 h of secondary growth shows maximum intensity at ~34°, as expected. These observations further verify the preferred *c*-orientation of the grains and confirm the increase in the degree of orientation for longer secondary growth time and larger thickness.

From the SEM cross sections of Figure 1b−d and the resulting Figure 1e it is indicated that uniform grain growth takes place. Furthermore, there is no induction time, indicating that the presence of seeds, under these secondary growth conditions, leads to elimination of the nucleation stage. This observation is different from our previous report[20] where calcined self-supported silicalite/alumina seed layers were used. In that case, an induction time for secondary growth was observed, and only a fraction of the precursor layer was covered initially with growing grains. Here, when the uncalcined/alumina-free precursor layer is brought in contact with the secondary growth solution, the high density and active external surface of grains allows for uniform growth. The seed crystals, at the early stages begin to grow in all possible directions. Under these conditions, growth of the existing particles contributes to film growth without incorporation of crystals nucleated in the solution, suggesting that grain growth proceeds by direct growth of the seeds of the precursor layer resulting in well-intergrown films, as shown by the SEM top views in Figure 1b−d.

The growth of the seeds propagates with time as a moving front from the precursor layer to the solution, as can be seen from the SEM cross sections in Figure 1b−d. Grains continue to grow as the film thickens and the crystal direction with the highest vertical growth velocity dominates, resulting in a columnar film texture. The rest of the grains that grow faster in a direction other than the vertical become buried. In the final films, grains have increasing size from the bottom to the top of the film and individual grains can be traced following the direction normal to the substrate. This can be clearly seen from the SEM cross section in Figure 1d for the thick film obtained after 15 h of secondary growth.

3.2. Secondary Growth at 140 °C. The effect of temperature variation on film growth rates during secondary growth was examined over a range of temperatures from 90 to 175 °C. The growth rate increased with increasing temperature. Initial growth rates were determined from the slopes of the growth curves and ranged from 0.01 μm/h at 90 °C to 0.84 μm/h at 175 °C. From these rates, the apparent activation energy for secondary growth was found to have a value of 70 ± 10 kJ/mol.

For secondary growth at the highest temperature of 175 °C, the high growth rate was sustained for 15 h and led to the formation of the thickest film (~13 μm), without observing pronounced surface roughening. For secondary growth at 140 °C, the growth rate was sustained for 20 h and SEM observation showed similar columnar film microstructure (Figure 4).

Although SEM observation showed similar columnar film microstructure, XRD from the films obtained at 140 °C revealed different orientation than the one of the films grown at 175 °C. The thin film and $\theta/2\theta$ diffractograms for up to 20 h of secondary growth at 140 °C are presented in Figure 5a−e. From Figure 5a−d it can be seen that the degree of orientation increases with time (or thickness) as in the case of secondary growth at 175 °C. Deviations from random orientation appear after 4 h (Figure 5b) and are strongly manifested after 9 h. Between 9 and 20 h (Figures 5d and 5e, respectively), although film thickness increases, the degree of out-of-plane orientation does not seem to change significantly. Moreover, the peak corresponding to the (002) reflection that was dominant for the films at 175 °C (Figure 2) has a small intensity for up to 20 h of secondary growth at 140 °C. Instead the (101) or (011) reflection is dominating, which suggests that the long axis of the columnar grains is not the *c*-axis, but their *c*-axis is tilted to an angle of 34° with respect to the direction normal to the substrate.

Additional support for this suggestion was provided from X-ray pole figure analysis, performed around the

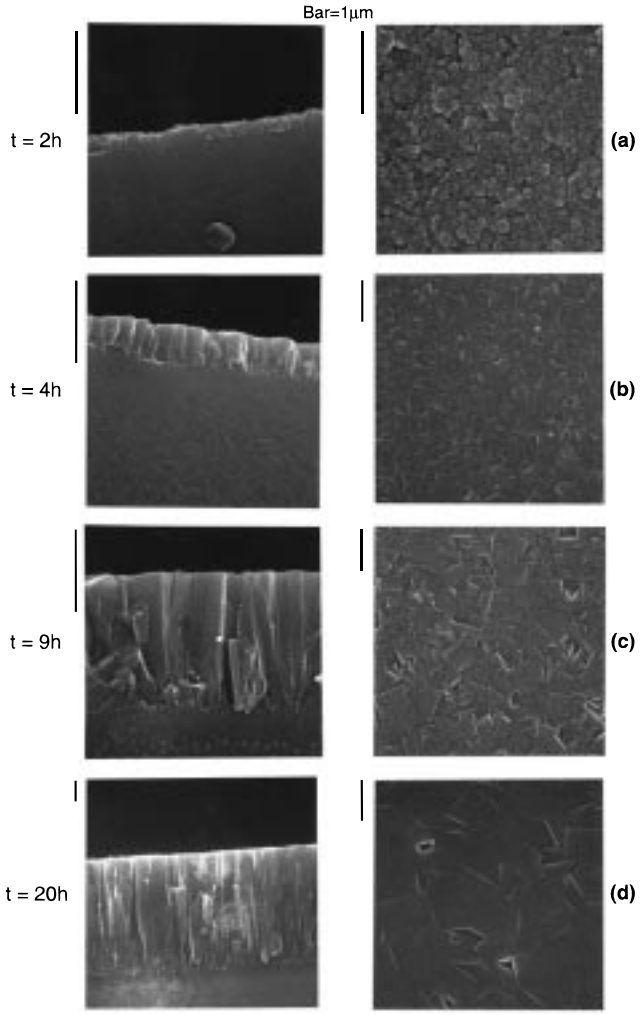

Figure 4. SEM micrographs for films obtained after secondary growth at 140 °C for (a) 2 h, (b) 4 h, (c) 9 h, and (d) 20 h.

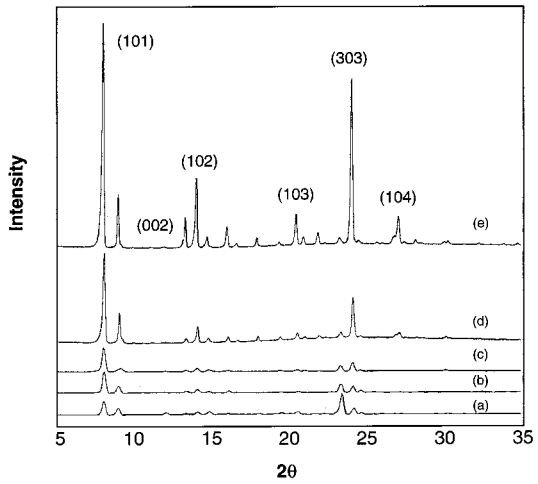

Figure 5. XRD patterns for secondary growth at 140 °C. Thin-film XRD for films obtained after secondary growth for (a) 2 h, (b) 4 h, and (c) 6 h and XRD for films after (d) 9 h and (e) 20 h.

(101) or (011) reflection (Figure 6) for films obtained after 9 and 20 h of secondary growth at 140 °C. These line plots show maximum intensity at 0° angle, which suggests that the columnar grains have their *c*-axis tilted 34° with respect to the normal. It is thus shown that secondary growth at 140 °C leads to a different out-

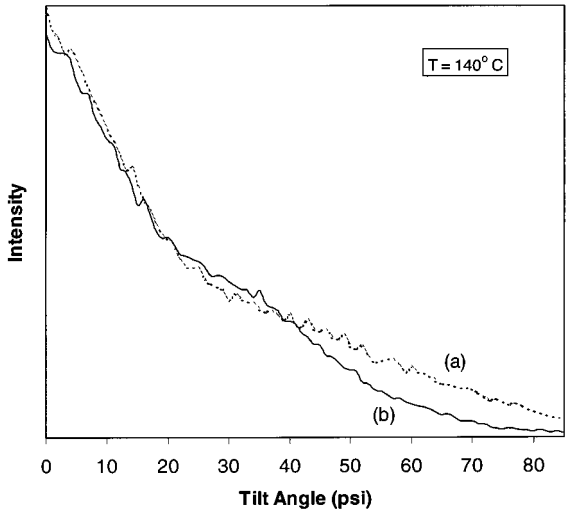

Figure 6. Pole figure line plots of the (101) reflection for films obtained after secondary growth at 140 °C for (a) 9 h and (b) 20 h.

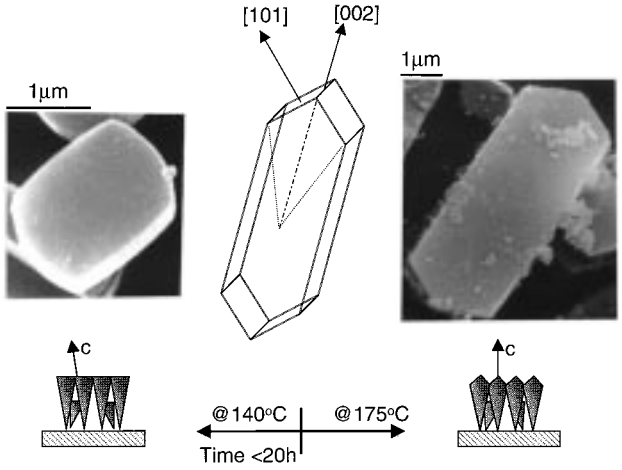

Figure 7. SEM images of MFI crystal grains in solution under conditions of secondary growth at 140 °C and 175 °C, and schematic illustration of proposed relation with film texture.

of-plane preferred orientation compared with secondary growth at 175 °C.

A possible explanation for the influence of temperature of secondary growth on film orientation is illustrated in Figure 7. As can be seen from the SEM micrographs in this figure, lower temperatures and short times favor the formation of more equiaxed MFI particles. On the other hand, at higher temperatures (e.g., 175 °C) elongated coffin-shape particles are obtained more quickly. Consequently, secondary growth at 175 °C leads to *c*-out-of-plane grain orientation, whereas deviations from this orientation occur at lower temperatures. More specifically, growth at 140 °C results in [*h*0*h*] orientation for secondary growth times up to 20 h. However, for longer secondary growth at 140 °C, this preferred orientation is not sustained and instead *c*-orientation starts to dominate as illustrated later.

As can be seen from Figure 8 for secondary growth at 140 °C, the film thickness initially evolves with time at a constant rate, which is sustained and increases although the silica concentration in solution decreases. After 20 h, the growth rate drops, presumably due to further nutrient depletion, leading to concentrations in

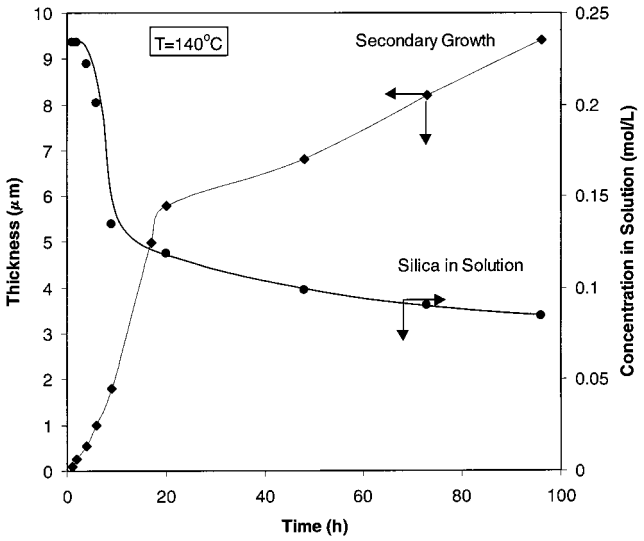

Figure 8. Film thickness evolution and silica depletion in solution for secondary growth at 140 °C.

the secondary growth solution that are not high enough to provide the necessary precursors. After the point where the growth rate at 140 °C declines, SEM observation indicates that faceting of the crystals dominates, resulting in surface roughening (Figure 9a). The surface roughening is accompanied with loss of preferred orientation. The $\theta/2\theta$ diffractogram corresponding to a film with thickness of ~9 μm that was obtained after 96 h is presented in Figure 9b. It can be seen from this figure that the same reflections are still present as in the case of secondary growth for up to 20 h at 140 °C (Figure 5). However, the intensity of the (002) reflection has increased significantly in this case. The associated (101) pole figure line plot (Figure 9c) shows a distribution with two maxima, one at 0° and the second at ~34° tilt angle. These observations suggest that for prolonged secondary growth at 140° the [*h*0*h*] preferred orientation cannot be sustained.

3.3. Sustained Growth. It was possible to sustain the initial growth rate by replenishing the nutrients in the solution. This replenishment was achieved by performing sequential secondary growth experiments at 140 °C, where the solution was renewed in time intervals from 5 to 15 h. The film thickness evolution during sustained growth is presented in the diagram of Figure 10a, and shows that the growth rate remained constant and equal to the initial growth rate. The final film had a thickness of ~ 8.5 μm after 50 h total time of secondary growth. The XRD and the pole figure line plots for this film are presented in Figures 10b and 10c, respectively. From Figure 10 it is clear that the [*h*0*h*] orientation that could not be preserved after 20 h of secondary growth at 140 °C can be sustained and

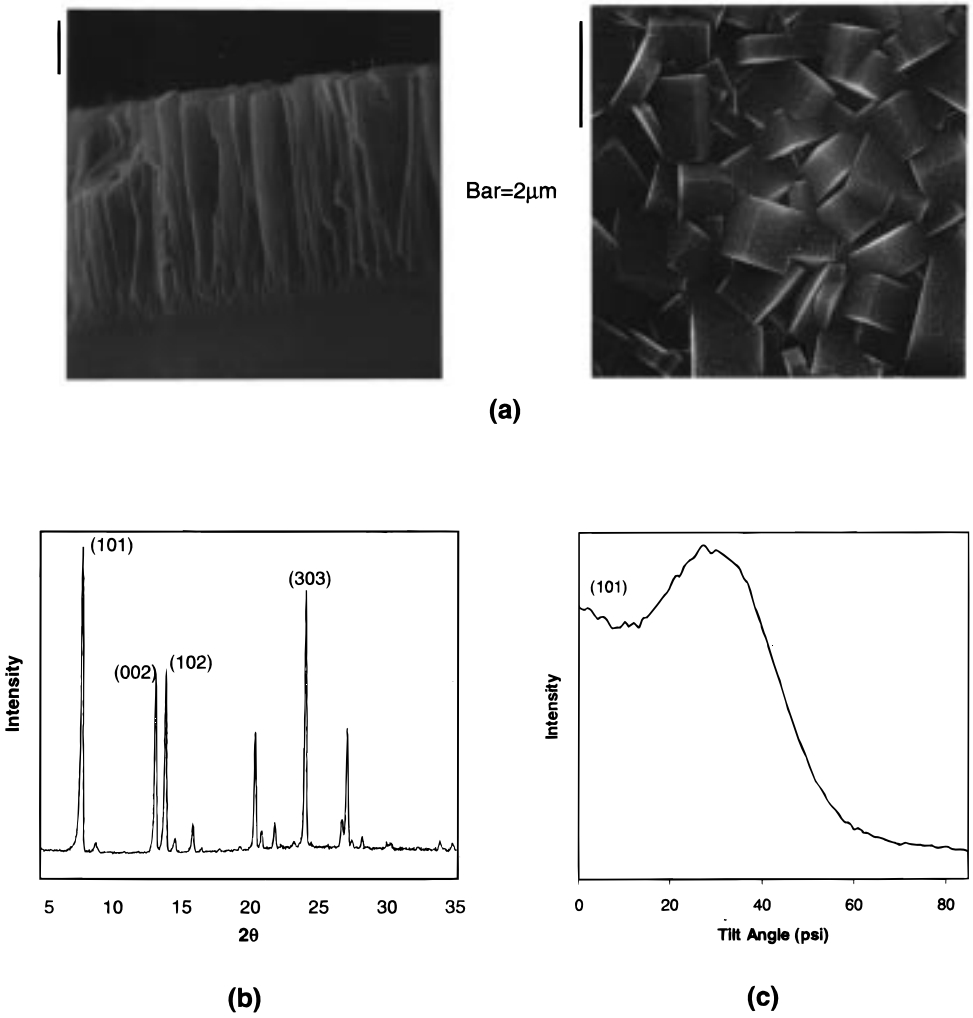

Figure 9. (a) SEM views for films obtained after secondary growth at 140 °C for 96 h; (b) corresponding XRD pattern; and (c) (101) pole figure line plot.

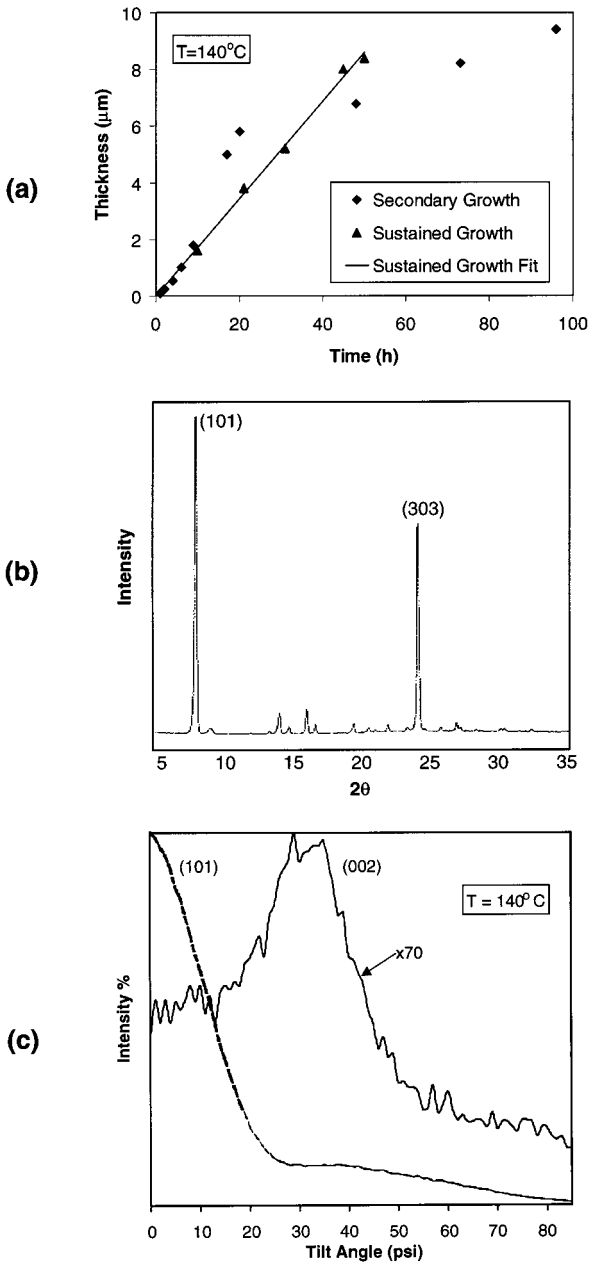

Figure 10. (a) Film thickness evolution under sustained secondary growth at 140 °C; (b) XRD pattern; and (c) pole figure line plot for a film obtained after sustained growth at 140 °C for 50 h.

enhanced using sequential renewal of reactants. The line plots corresponding to the (101) and (002) pole figures shown in Figure 10c indicate that the grains are aligned with the *c*-axis to an angle of ~34° to the direction normal to the substrate.

3.4. Transparent and Oriented MFI Films. The films prepared by sustained growth at 140 °C exhibit, in addition to preferred orientation, small surface roughness (~0.1 μm) and well intergrown columnar microstructure. As a result, these oriented films even at thickness (~10 μm) well exceeding the wavelength of visible light are optically transparent. The transparency is illustrated in Figure 11, where a picture of a film grown on a glass slide is presented. The left area that appears darker is the one that was not coated with precursor layer. During secondary growth crystals nucleated in the solution or at the solution−substrate

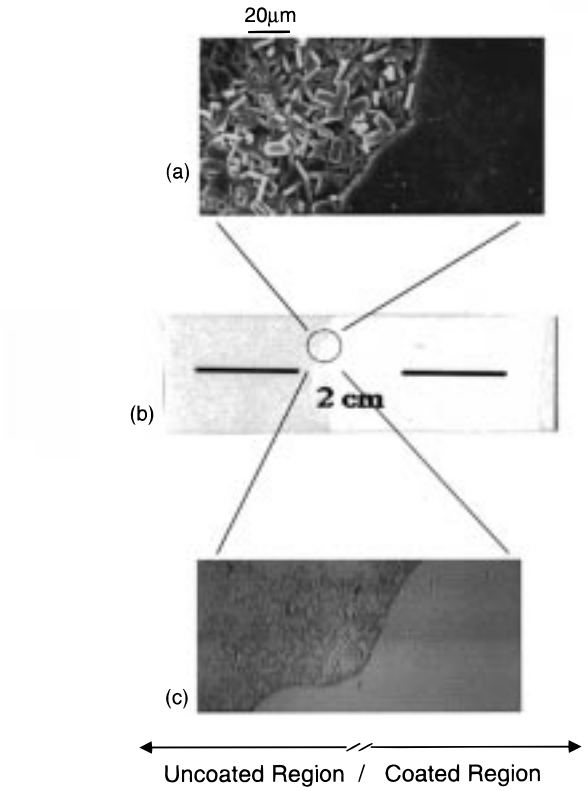

Figure 11. (a) SEM top-view and (c) optical micrograph from the interface of the coated with precursor layer and uncoated regions of the substrate (b) after secondary growth.

interface were deposited in this area. The nonuniform microstructure results in considerable scattering of visible light (SEM and optical micrographs in Figure 11a and c). In contrast, a very smooth film occupies the area initially covered with the precursor layer. Optical inspection of the coated part of the glass substrate after secondary growth does not reveal any difference from the as received glass slides, whereas the uncoated part appears nearly white.

The microstructural control demonstrated here is also of significance for the use of these films in equally important applications, such as membranes for gas separations and coatings on sensors. Similar film microstructures have been obtained under similar secondary growth conditions on porous alumina disks and silicon wafers. The results reported point to the search of secondary growth conditions leading to slower nucleation compared with growth rates and highly anisotropic growth rates with fastest growth along the direction that is desired to dominate the out-of-plane orientation. The emphasis was on secondary growth conditions, whereas no attempt was made in changing the orientation or density of the precursor layer. As is shown elsewhere,[36] the density of seeds and their orientation can play an important role in determining the final film microstructure.

4. Conclusions

Polycrystaline MFI films were prepared by secondary growth of precursor layers. Precursor layers that

(36) Boudreau, L. C.; Kuck, J. A.; Tsapatsis, M. *J. Membr. Sci.* In press.

adhere on the substrate can be formed without calcination or use of surface modification or additives. During secondary growth, the precursor particles remain attached on the surface. Secondary growth conditions were identified where film growth proceeds by direct growth of the seed particles, leading to continuous columnar films with single grains extending along the film thickness.

This work demonstrates that orientation of molecular sieve films can be manipulated by secondary growth conditions, as illustrated by the preparation of the *c*-oriented ([00*l*]), and the [*h*0*h*]-oriented films. Moreover, it is shown that secondary growth can be sustained upon repeated renewal of reactants, providingcontrol over film thickness while preserving the preferred orientation and surface smoothness.

To our knowledge, this work for the first time demonstrates combined microstructural control over film thickness, uniformity, surface roughness, crystal orientation, continuity, and intergrowth for molecular sieve films.

Acknowledgment. Support for this work was provided by NSF [CTS-9624613 (CAREER) and CTS-9512485 (ARI)] and NETI. M.T. is grateful to the David and Lucile Packard Foundation for a Fellowship in Science and Engineering.

CM9802402